IJCRT.ORG

ISSN: 2320-2882

c208



INTERNATIONAL JOURNAL OF CREATIVE RESEARCH THOUGHTS (IJCRT)

An International Open Access, Peer-reviewed, Refereed Journal

Magneto Optical Properties Of Ferromagnetic Full Heusler Compounds

¹Poonam Singh, ²Dr Chandravir Singh, ³Dr Ajay Singh Verma

¹PhDResearch Scholar, ²Professor

Department Of Physics,

Agra College, Dr. Bhimrao Ambedkar University, Agra (UP), India

ABSTRACT:

The structural, electronic, magnetic, and optical properties of the full-Heusler compounds Co₂MnZ (where Z = As, Al, Sb, and Sn) have been studied using the Perdew Burke Ernzerhof (PBE) exchange correlation functional of the Generalized Gradient Approximation (GGA) and the ultra soft pseudo potential USP plane wave based on density functional theory (DFT). The results demonstrate that both compounds have a cubic structure and are in a stable condition. The mechanical stability requirements are also satisfied by the computed elastic constants. In comparison to their antiferromagnetic or nonmagnetic phases, these compounds' ferromagnetic phases exhibit greater stability due to their type's most stable structure. There are four interpenetrating fcc sub lattices in this structure. Of which two are part of the same element. An unique special class of materials described by heusler is lie at the edge of compounds and alloys, but combining the features of both.

Keywords: Electronic, Magnetic and Optical Properties, Density Functional Theory, full Heusler alloys.

INTRODUCTION:

Recent research has examined the structural, electrical, and optical characteristics of Co₂MnAs and Co₂MnSb. GGA-PBE procedure, which is designed using DFT and integrated into the CASTEP code, is used for calculations. A few half-metallic ferromagnetic materials find application in spin valves [1–5]

due to the elevated Curie temperature. [7-9] Spintronics devices are used in many solid-state devices such as magnetic sensors, memory storage, spin filters, spin valves, and tunneling magneto resistance (TMR) phenomena [11–13]. [14, 15] Adopting spintronics devices has advantages in terms of faster data processing and less power consumption. The Fm-3m space group contains the Full-Heusler alloys' L21 structure. This construction's elements are all positioned on one of the four fcc lattices that are penetrated in the direction of the principal diameter. Z is one of the sp elements from the major group III-V elements, whereas X and Y are transition metal elements. Full-Heusler materials frequently contain the formula X₂YZ. Throughout two of these fcc sub lattices one of them and another are the X, Y, and Z elements found in this structure. Optoelectronics and spintronics components heavily rely on their dielectric, optical, electrical, and structural characteristics. [16-21] Numerous research projects have been undertaken on various attributes and uses. Regarding spintronics, Utilizing a first-principles approach with the full potential linearized augmented plane-wave (FP-LAPW) method and the generalized gradient approximation plus U (GGA + U), the electronic, magnetic, and optical characteristics of the Co₂MnAs full-Heusler compound have been computed. The outcomes are contrasted with other Co₂MnZ full-Heusler compound attributes (where Z = As, Al, Ga, and Sn). Co₂MnAs is a half-metallic ferromagnetic compound with 100% spin polarization at the Fermi level, according to the results of our computations. The Co₂MnAs compound's halfmetallic gap and total magnetic moment are determined to be 0.43eV and 6.00 lB, respectively.

The spin wave stiffness constant and Curie temperature of the Co₂MnAs compound are also expected to be approximately 3.99meV nm2 and 1109 K, respectively. The optical data demonstrate that the system's interactions with free electrons are what cause the prevailing behavior at energies lower than 2eV. The imaginary component of the dielectric function and an examination of key locations in the second energy derivative of the dielectric function have been used to compute inter band optical transitions. The results demonstrate that the Co₂MnAs compound has many plasmon energies, the highest of which is observed at 25eV. Calculations are also performed for Co₂MnAs refractive index fluctuations and optical reflectivity for radiation at normal incidence. Co₂MnAs is an excellent choice for usage in spintronic components and magneto optical devices due to its strong magnetic moment, high Curie temperature, 100% spin polarization at the Fermi level, and optical qualities.

1. Computational methodology:

The structural, electrical, and half-metallic characteristics of the Co_2MnZ full-Heusler alloys (Z=As, Sb, Ga, and Sn) are obtained by using density functional theory (DFT) with the GGA [22.23]. Co2MnAs full-Heusler compounds have received less research attention than other Co-based Heusler alloys. The optical characteristics of this compound and other Co_2MnX full-Heusler compounds have not been reported often, as far as the authors are aware. This work used the full-potential linearized augmented plane-wave (FP-LAPW) method and the generalized gradient approximation plus U (GGA + U) to compute the electronic, magnetic, and optical properties of the Co_2MnAs full-Heusler compound from first principles. The outcomes are also contrasted with other Co_2MnZ (Z=Sb, Ga, Al, and Sn) compound characteristics.

RMT (a.u.) Compounds Co₂MnAs Co₂MnAl Co₂MnGa Co₂MnSn Co 2.39 2.18 2.19 2.35 2.19 2.08 2.09 2.34 Mn \mathbf{Z} 2.28 1.81 2.08 2.46

Table 1. Muffin tin radius (RMT) for Co_2MnZ (Z = As, Al, Ga, Sn).

2. Results and discussion:

2.1 Electronic Properties:

As a function of the unit cell volume, the energy of Co₂MnAs was determined. A Birch–Murnaghan equation of state fit was applied to the collected data. Calculating the equilibrium volume and lattice constant required using the equation of state. Figure 1 illustrates how the internal energy varies with unit cell volume. The equilibrium lattice constant that was computed was 5.70 A. In addition, the equilibrium volume's total energy of Co₂MnAs in nonmagnetic, ferromagnetic, ferrimagnetic, and antiferromagnetic structures was computed; the resulting values were 12,413.279364Ry, 12,413.398722Ry, 12,413.364517Ry, and 12,413.363353Ry, respectively. The ferromagnetic state was shown to have a higher probability of developing than the other states because of its energy value. Investigating all of the optical, magnetic, and electrical characteristics was done withto determine the equilibrium lattice constant, the variation of the internal

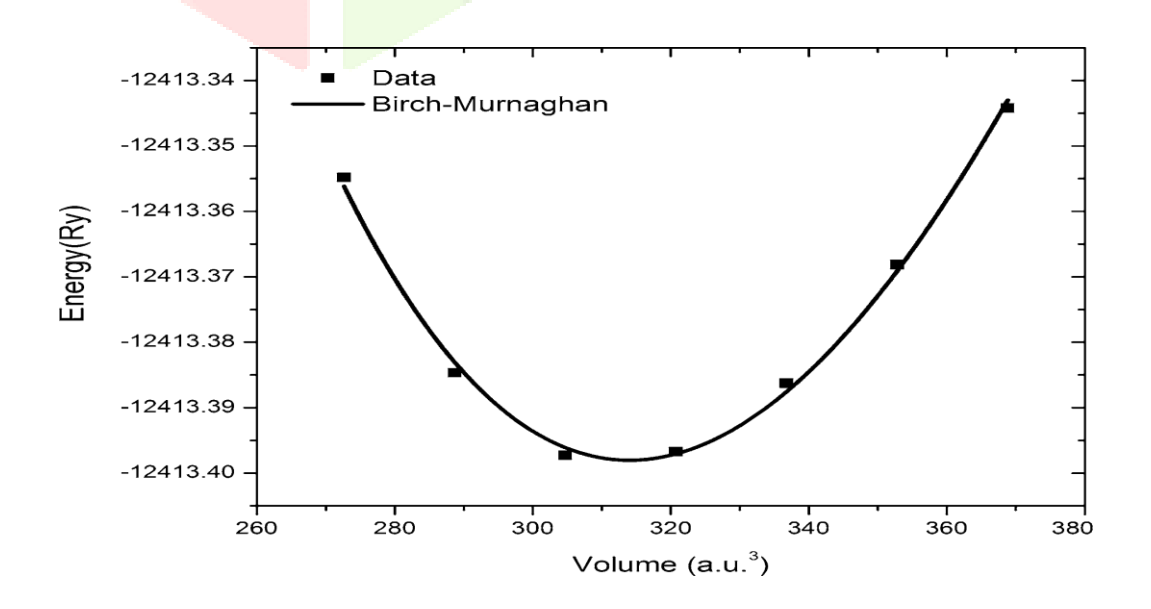


Fig. 1. Variation of internal energy of Co₂MnAs compound as functionofunitcellvolumein Ferromagnetic

IJCRT2409250 International Journal of Creative Research Thoughts (IJCRT) www.ijcrt.org c210

First Ideas Prediction of Co₂MnAs Full-Heusler Half-Metallic Compound's Electronic, Magnetic, and Optical Properties. In the energy range of 8.0eV to 8.0eV, the total and partial density of states (T-DOS and P-DOS) for the up- and down-spin channels of the Co2MnAs molecule are displayed in Figure 2. It is evident that there is a discrepancy in the T-DOS between the up- and down sell channels. Consideration of the up-spin channel reveals that the Co₂MnAs compound has occupied states at the Fermi level as well. The system behaves metallically under these conditions. In contrast, Co₂MnAs exhibits semiconducting behavior for the down-spin channel and contains unoccupied states at the Fermi level. Between the lowest empty state and the highest occupied state in the case of down-spin states.



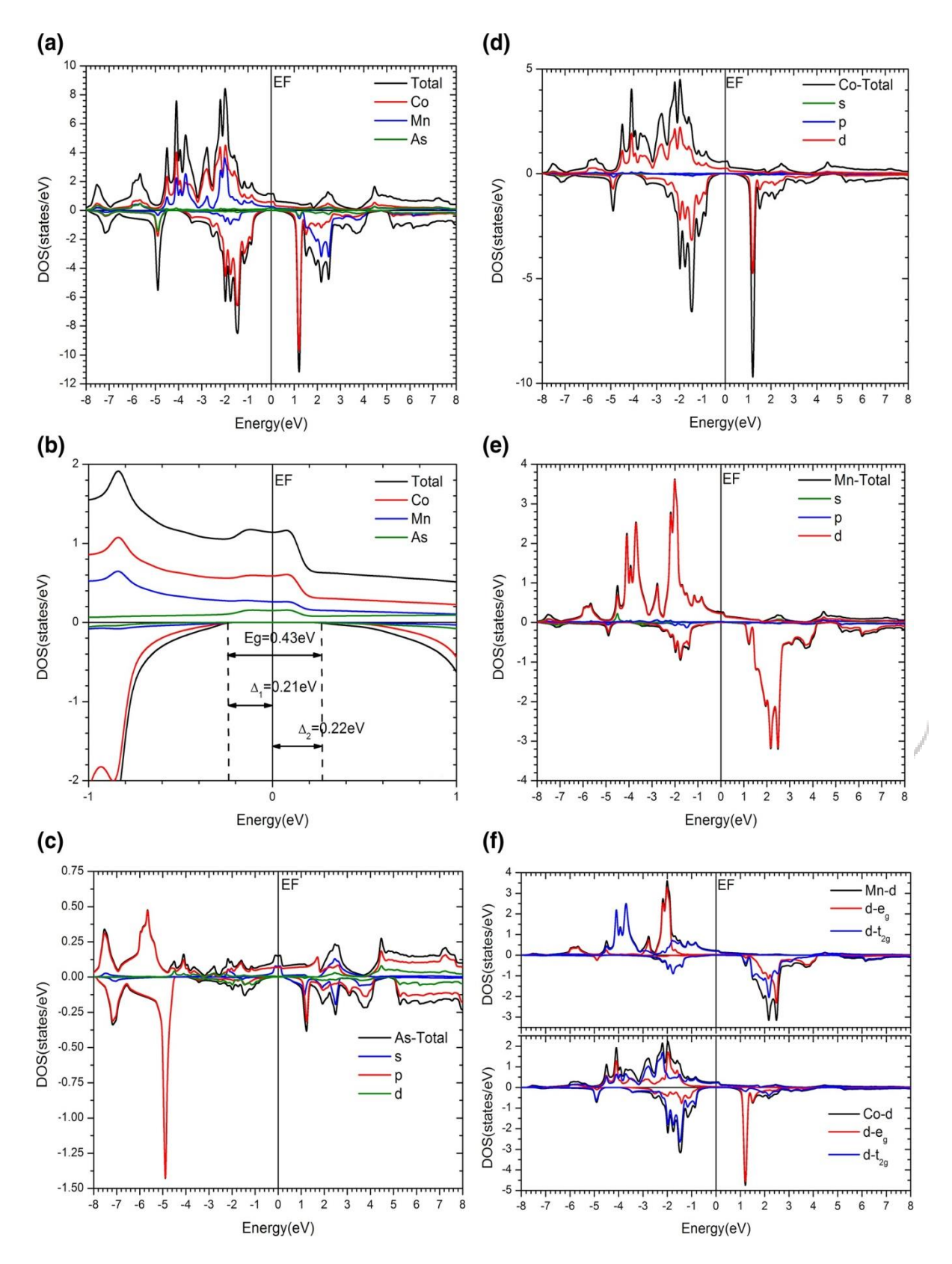


Fig.2.Total and partial density of states of Co_2MnAs compound in energy range between 8.0eV and 8.0eV. Solid line shows Fermi level. (a) Total density of states of Co_2MnAs compound with contribution of each atom.(b)Half-metallic energy gap in down-spin channel.(c) Partial DOS of As atom.(d) Partial DOS of Co atom.(e) Partial DOS of Mn atom.(f) Comparison between density of states for de_g and dt_{2g} orbital of Co and Mn atoms.

a half-metallic band gap of roughly 0.43 eV exists. For the down-spin channel, the energy gaps are 0.21 eV and 0.23 eV, respectively, between the highest occupied state and the Fermi level (D1) and the lowest unoccupied state and the Fermi level (D2). Atoms of Co, Mn, and As contribute mostly to the DOS at the Fermi level. For additional research, the band structure of Co₂MnAs is displayed in Fig. 3.

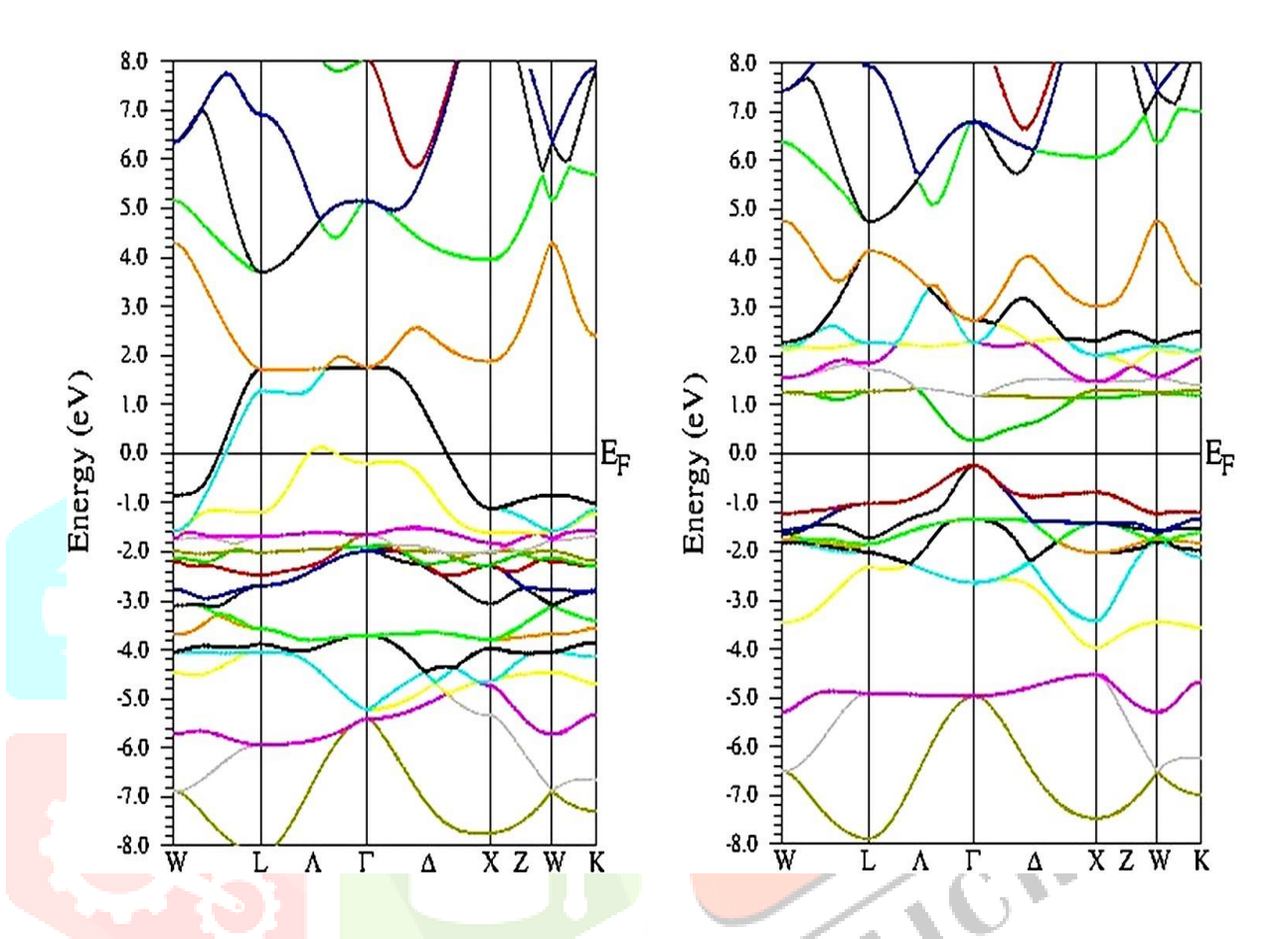


Fig.3.BandstructureofCo₂MnAsfordown-spin(rightfigure)andup-spin(leftfigure)channel.

Co and Mn atoms contribute significantly to the DOS over the majority of the energy range. The contribution of As atoms becomes similar to that of Mn and Co atoms in the energy range of 8eV to 4eV. As p orbitals is responsible for this contribution. D-orbitals are the primary source of the Co and Mn atoms' contribution to the DOS. Mn and Co atoms' d-orbitals are divided into two degenerate groups, deg and d t2g, which have double and triple accordingly, degeneracy. The development of various hybrid and nonhybrid states results from hybridization between d eg and d t2g orbitals in the Co-Co plane and Mn d-orbitals with As p-orbitals in the Mn-As plane. The source of the energy gap in the down-spin channel is the energy differential between the hybrid and non-hybrid states.

2.2 Magnetic Properties

Localized and delocalized magnetism, ferromagnetism, anti ferromagnetism, and ferrimagnetism are just a few of the magnetic characteristics that Heusler alloys display [24–27]. A weak applied magnetic field causes Heusler alloys, which are frequently ferromagnetic, to saturate. [28] When Mn atoms are the sole ones in an X₂MnZ combination with a magnetic moment, antiferromagnetic characteristics typically result.

In Heusler alloys, ferrimagnetic order is much rarer than ferromagnetic and antiferromagnetic order[28]. Most metals exhibiting local moment behavior are alloys, which fall into one of two categories: ordered or disordered. Ordered systems include Heusler alloys [28]. The local behavior of the magnetic moments is described based on the density of states and Kubler et al. [29]. In the DOS of Co₂MnAs, the Mn 3d and Co 3d states are almost filled in the up-spin channel, but the down-spin Mn 3d orbitals are almost empty. As a result, hybridization between Mn 3d orbitals and Co 3d orbitals in the up-spin channel forms a d-band, which is a combination of both atoms; however, in the down-spin channel, Mn 3d orbitals are almost empty and do not participate in hybridization, which results in the formation of a magnetic localized area. The values of the total magnetic moment and magnetic moment for each atom in Co₂MnAs compound are summarized in Table I, in comparison with other Co-based alloys.

2.3 Optical Properties

To determine the response to an applied electromagnetic wave, the dielectric function of the material is usually calculated. The dielectric function is complex,

denoted as
$$e(x) = e_1(x) + ie_2(x). e_1(x)$$

Where is the real part and $e_2(x)$ is the imaginary part of the dielectric function. The dielectric function consists of two contributions (interband and intraband). The intraband contribution need only be considered form metals at low energy. Figure 4 shows the variation of the real and imaginary parts of the dielectric function and energy loss function in L(x) for Co_2MnAs in terms of incident photon energy. At low energies, $e_1(x)$ tends to large negative values and $e_2(x)$ tends to large positive values. This feature is one of the characteristics of intraband transition in metals. It is well known that metals have large negative values of $e_1(x)$ at low energies, which is due to the mechanism of free electrons, while positive $e_1(x)$ is usually related to interband transitions of bonding electrons. [30] $e_1(x)$ starts from large negative values and reaches zero at energy of 1.14eV at the first root. Roots of the real part of the dielectric function are physically important. In fact, in the energy range where $e_1(x)$ is negative, electromagnetic waves do not propagate and absorption and reflection processes are dominant. In the energy range where the dielectric function is positive, Co₂MnAs compound behaves like a dielectric. Moreover, if there is a significant peak in the energy loss function at energies related to the roots of the real part of the dielectric function, these roots determine the plasmon energies of the compound .It is clear from Fig.4 a that, at energy of 25eV, there is a prominent peak in L(x). This energy determines the energy of bulk plasmons in Co_2MnAs compound. In addition, L(x) and $e_1(x)$ at low energies are plotted in Fig.4b. It is observed that the energies of 1.14eV and 5.12 eV are also roots of the dielectric function . At these two roots, there is a relatively prominent peak in L(x). Therefore, it appears that Co₂MnAs compound has three plasmon energies. At low energies, these plasmon energies are due to presence off re electrons in the system .Peaks in the imaginary part of the dielectric function are related to interband and intraband transitions. These peaks are marked with lower case letters in Fig.4a. The large value of $e_2(x)$ is connected to the intraband transitions which occur at low energies. According to the band structure and density of states, itis possible to determine the relationship between the peaks of e₂(x) and related optical transitions. Major intraband transitions are attributed to the Mn 3d and Co 3d bands in the upspin channel which cross the Fermi level. Peaks a ,b, and c are related to the optical transitions of Co3d orbitals in the down-spin channel as well as Mn 3d orbitals to As p orbitals above the Fermi level. It seems that peaks d and e originate from Mn 3d and Co 3d in the up-spin channel to As p states. In the down- spin channel and below the Fermi level, peak f likely originates from As p transitions to Co 3d and Mn 3d orbitals. Further more the second derivative of the dielectric function also helps to explain the optical transitions, as shown in Fig. 4c.The predominant valleys are marked with arrows, being compatible with most of the optical transmissions (peaks specified in the imaginary part of the dielectric function). The roots of the real part of the dielectric function, the energy range in which the real part of the dielectric function is negative, the peaks of the imaginary part of the dielectric function, and the plasmonic energies are summarized in Table 2.

Table 2. Optimized parameters of Co_2MnZ (Z = As, Al, Ga, Sn).

	Lattice constants a ₀ (Å)		Bulk Modulus (GPa)		Equilibrium Energy (Ry)	Pressure derivative WIEN2k
Compounds	Calculated		Calculated			
	Wien2k	ATK	Wien2k	ATK		, , , , , , , , , , , , , , , , , , ,
Co ₂ MnAs	5.756	5.856	226	206	Co ₂ MnAs	5.756
Co ₂ MnAl	5.723	5.845	218	200	Co ₂ MnAl	5.723
Co ₂ MnGa	5.726	5.791	202	181	Co ₂ MnGa	5.726
Co ₂ MnSn	5.751	5.784	234	207	Co ₂ MnSn	5.751

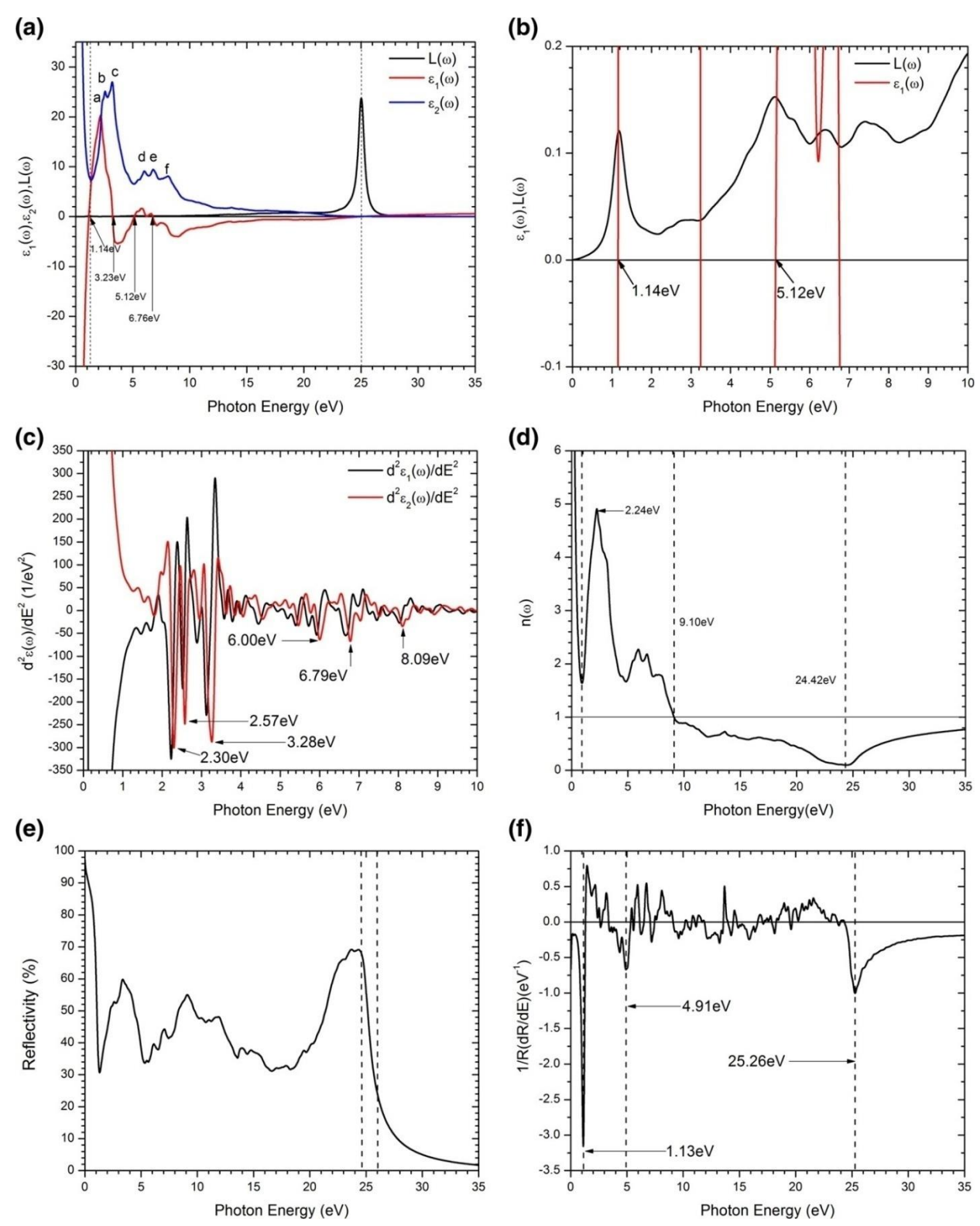


Fig. 4. (a) Variations of real and imaginary parts of dielectric function, and energy loss function in terms of photon energy. (b) Real part of dielectric function and energy loss function in terms of photon energy in energy range between 0eV and 10eV. (c) Second energy derivative of dielectric function.(d) Refractive index of Co₂MnAs compound in terms of incident photon energy.(e) Optical reflectivity of Co₂MnAs compound in terms of incident photon energy in first energy derivative of optical reflectivity

The optical reflectivity of Co₂MnAs compound as a function of photon energy is shown in Fig. 4e. At low energies, the reflectivity of Co₂MnAs is high and the compound is almost a 100% reflector. With increasing photon energy, the reflectivity reduces sharply to approximately 30%

over a range of 1eV. In the range from 1eV to 25eV, the reflectance varies from 30% to 70%. At energy near 25eV, the reflectance is close to zero. For further discussion, the energy derivative of the reflectivity is shown in Fig. 4f. It is observed that There is a significant singularity at energy of 1.13eV,4.91eV,and 25.26eV, which are all near plasonic energies of Co₂MnAs.

2.4 Summary and Conclusions:

Based on density functional theory (DFT) and the full potential linearized augmented planewave (FP-LAPW) method, the optical, magnetic, and electronic properties of Co₂MnAs full-Heusler compound were studied .The electronic results show that Co₂MnAs compound is a half-metal with 100% spin polarization at the Fermi level. The half-metallic energy gap is equal to 0.43eV in the down-spin channel, being due to hybridization of bonding and non hybrid states between Co, Mn, and As atoms. The Fermi level is located approximately at the middle of the energy gap. The magnetic properties of Co₂MnAs compound reveal a total magnetic moment of $6.00l_B$, higher than for other Co_2MnZ (Z = Al, Ga, Sn, Sb) compounds (except sb). In addition, compared with other Co₂MnZ Heusler compounds, it was observed that the role of the Z atoms in the magnetic moment of Co and Mn is important. Based on their relationships with the total magnetic moment in Co₂MnZ compounds, the Curie temperature and spin-wave stiffness of Co₂MnAs were predicted to lie near 1109 K and 3.99 meVnm², respectively. The dominant behavior in the optical properties of Co₂MnAs compound at low energy (below2eV) is due to the mechanism of free-electron interactions in the system. The interband optical transitions were analyzed based on the imaginary part of the dielectric function, critical points in the second derivative of the dielectric function, and the DOS. A strong plasmon energy was found at 25eV for Co₂MnAs compound, and two other plasmon energies at 1.14eV and 5.12eV. Investigations of the refractive index and optical reflectivity of Co₂MnAs compound suggest that the super luminal phenomenon occurs around energy equal to 9.10eV and the minimum refractive index occurs near the plasmon energy of 25eV. It was observed that a significant drop in the optical reflectivity occurs near the plasmonic energies of Co₂MnAscompound.

REFERENCES:

- [1]. N.R. Checca, R.J. Caraballo- Vivas, R. Torrao, A. Rossi, and M.S. Reis, Mater. Chem. Phys. 196, 103 (2017).
- [2]. B. Balke, G. Fecher, and C.Felser, Spintronics (Dordrecht: Springer, 2013), pp. 15–43.
- [3]. Y.Z. Abdullahi, T.L. Yoon, M.M.Halim, M.R. Hashim, and T.L. Lim, Surf. Sci. 667, 112 (2018).
- [4]. G. Torosyan, S. Keller, L. Scheuer, R. Beigang, and ETh Papaioannou, Sci. Rep. 8, 1311 (2018).
- [5]. S.A. Khandy, I. Islam, D.C. Gupta, and A. Laref, J. Solid State Chem. 270, 173 (2019).
- [6]. G.Y. Gao, K.L. Yao, E. Sasioglu, L.M. Sandratskii, Z.L. Liu, and J.L. Jiang, Phys. Rev. B 75, 174442 (2007).
- [7]. M. Moradi, M. Rostami, and M. Afshari, Can. J. Phys. 90, 531 (2012).
- [8]. G.Y. Gao, K.L. Yao, M.H. Song, and Z.L. Liu, J. Magn. Magn. Mater. 323, 2652 (2011).
- [9]. M. Rostami, M. Afshari, and M. Moradi, J. Alloys Compd. 575, 301 (2013).
- [10]. S. Berri, D. Maouche, M. Ibrir, and B. Bakri, Mater. Sci. Semicond. Process. 26, 199 (2014).
- [11]. J. Atulasimha and S. Bandyopadhyay, Nanomagnetic and Spintronic Devices for Energy-Efficient Memory and Computing (New York: Wiley, 2016), pp. 3–7.
- [12]. A. Bsiesy, C. R. Phys. 6, 1022 (2005).
- [13]. R.A.P. Ribeiro, A. Camilo, and S.R. De Lazaro, J. Magn. Magn. Mater. 394, 463 (2015).
- [14]. M.N. Baibich, J.M. Broto, A. Fert, F. Nguyen Van Dau, F. Petroff, P. Etienne, G. Creuzet, A. Friederich, and J. Chazelas, Phys. Rev. Lett. 61, 2472 (1988)
- [15]. G. Binasch, P. Grunberg, F. Saurenbach, and W. Zinn, Phys. Rev. B 39, 4828 (1989).
- [16]. F. Belkharroubi, M. Ameri, D. Bensaid, Structural, Magnetic, Electronic and Mechanical Properties of Full-Heusler Alloys Co2YAl (Y= Fe, Ti): First Principles Calculations with Different Exchange-Correlation Potentials. J. Magn. Magn. Mater. 448, 208 (2018).
- [17]. M.H. Elahmar, H. Rached, and D. Rached, The Half Metallic Feature at High Temperature of the Novel Half-Heusler Alloys and Their [100] Oriented Layered Superlattices: A DFT Investigations. Mater. Chem. Phys. 267, 124712 (2021).
- [18]. H. Saib, S. Dergal, H. Rached, and M. Dergal, Spin Gapless Semiconductor Behavior in d°-d Half-Heusler CrSbSr: Potential Candidate for Spintronic Application. SPIN 10, 2050025 (2020).
- [19]. P.K. Kamlesh, R. Gautam, S. Kumari, and A.S. Verma, Investigation of Inherent Properties of XScZ (X = Li, Na, K; Z = C, Si, Ge) Half-Heusler Compounds: Appropriate for Photovoltaic and Thermoelectric Applications. Phys. B: Condens. Matter. 615, 412536 (2020).
- [20]. T. Zerrouki, H. Rached, D. Rached, M. Caid, O. Cheref, and M. Rabah, First-Principles Calculations to Investigate Structural Stabilities, Mechanical and Optoelectronic Properties of NbCoSn and NbFeSb Half-Heusler Compounds. Int. J. Quantum Chem. 121, 26582 (2020).

c218

- [21]. F. Parvin, M.A. Hossain, First-Principles Calculations to Investigate Mechanical Optoelectronic and Thermoelectric Properties of Half-Heusler p-Type Semiconductor BaAgP. Res. Phys. 23, 104068 (2021)
- [22].A.D. Becke, J. Chem. Phys. 140, 18A301 (2014)
- [23]. J.P. Perdew, K. Burke, and M. Ernzerhof, Phys. Rev. Lett. 77, 3865 (1996)
- [24].P.J. Webster and K.R.A. Ziebeck, Landolt-Bornstein, NewSeries Group III,ed .H.P.J. Wijn (Berlin:Springer,1988), p.75
- [25]. P.J. Webster, K.R.A. Ziebeck, and K.U. Neumann, Landolt-Bornstein, New Series, Group III, Vol. 32, ed. H.P.J. Wijn(Berlin:Springer,2001),p.64414.
- [26]. J. Pierre, R.V. Skolozdra, J. Tobola, S. Kaprzyk, C. Hord-equin M.A. Kouacou, I. Karla, R. Currat, and E. Lelievre-Berna, J. AlloysCompd. 262, 101(1997).
- [27]. J.TobołaandJ.Pierre, J.Alloys Compd. 296, 243 (2000).
- [28].E.Şaşioğlu, First-Principles Study of the Exchange Inter-actions and Curie Temperature in Heusler alloys.Ph.D.
- [29]. J.Kübler, A.R. William, and C.B. Sommers, Phys. Rev. B 28,1745 (1983).
- [30]. M.M.Noskov,Optical and Magneto-optical Properties of Metals (Sverdlovsk:UNTS,1983),p.217.